Supporting information

High-flux charge transfer layer confers solid electrolyte interphase with uniform and rich LiF for stable lithium metal battery

Haijie Zhao[1], Yumeng Peng[1], Xianbin Liu[1,*], Shibo Du[1], Yiyao Yu[1], Ting Liu[1], Yanhong Yin[1], Sayed Y. Attia[2], Yesheng Li[1] and Ziping Wu[1,*]

* Corresponding author. E-mail address:

Xianbin Liu, *xianbin_liu@jxust.edu.cn*; Ziping Wu, *wuziping724@jxust.edu.cn*

Materials and Methods

Materials preparation: CNT powers were prepared by chemical vaper depostion and then purified with acid treatment and thermal treatment as reported in our published paper. Meanwhile, GO powers were prepared by improved Hummer method. Afterwards, CNT powers and GO powers were mixed with a constant proportion to form uniform slurry. The slurry was coating on a glass substrate to obtain GO/CNT film. Finally, GO/film was experienced by HI reducing and 2800 ℃ graphitized processing, to achieve the GrGO/CNT film. The thickness of GrGO/CNT film was ~8 μm.

Structure characterizations: The microstructure was observed by field-emission transmission electron microscopy (TEM, Tecani G2 F20, Japan). The surface and cross-section morphology was observed by field-emission scanning electron microscopy (SEM, Supra 55 ZEISS, Germany) and atomic force microscopy (AFM, MFP-3D-infinity, Asylum Research). The functional groups were detected by the Fourier-transform infrared Spectra (FTIR, Thermo Nicolet 5700), The crystal structures were analyzed with the X-ray diffraction (XRD, Rigaku Empyrean, Holland) using Cu-Ka radiation. The Raman spectra were detected by a Renishaw (Invia, England) with a wavelength of 532 nm. The element distribution was collected by a

Electron probe X-ray microanalyzer (EPMA, JXA-iSP100, Japan). The wettability was analyzed by a contact angle apparatus (JY-82A, China). The component analysis was carried out with a X-ray photoelectron spectroscopy (XPS, ESCALAB 250, USA). The specific surface area and pore size distribution were determined by Brunauer-Emmette-Teller (BET) theory.

Electrochemical test: Li stripping/depositing behaviors were investigated by galvanostatic technique using the Neware battery testing system (CT2001A, China) based on a symmetric cell. The symmetric cell was assembled using Li/HCTL electrodes as counter electrode and 1.0 M LiTFSI in DOL/DME (1,3-dioxolane/1,2-dimethoxyethane v/v=1) with 1 wt% $LiNO_3$ as electrolyte in an argon-filled glovebox with $H_2O < 0.01$ ppm and $O_2 < 0.01$ ppm. The Li/HCTL was prepared by coating GrGO/CNT film on the Li tablet. The current density was ranged from 1, 2.5, 5,10 mA cm^{-2} and the depositing capacity was 1, 2.5, 3 and 5 mAh cm^{-2}. The impedance analysis was conducted on an electrochemical station (Ivium, VMP-300, Netherlands) with a frequency of 10^5-10^{-2} Hz. The full battery was assembled with Li/HCTL anode and $LiCoO_2$ (LCO) cathode. The LCO cathode was prepared by the LCO: SPC: PVDF of 90: 6: 4. The loading mass of LCO was ~6.18 mg cm^{-2}. The galvanostatic charge/discharge (GCD) curves and cyclic voltammetry (CV) curves were tested. The specific capacity was calculated at different rates.

SEI analysis: Depth profiling was conducted on XPS using Ar ion sputtering for different times from 0 to 480 s at an accelerating voltage of 0.5 kV to a 0.5 μm depth. The thickness of SEI was measured by the TEM images. The spatial distribution of SEI was observed by Time-of-Flight secondary ion mass spectrometry (TOF-SIMS, TOF.SIM 5 GmbH, Germany). And the elasticity modulus and surface flatness was tested by a conducting atomic force microscopy (CAFM, MFP-3D-infinity, Asylum Research, Oxford). The ion conductivity of Li^+ for SEI was calculated through the following: $\sigma=2L/(R\cdot S)$. L is the thickness of SEI, and R is the electrochemical impedance, S is the electrode areal.

COMSOL simulation: Simulation of the Li plating morphological and concentration evolution was conducted using phase-field simulation in 4×3.5 μm^2 areas with an

electrodeposition time of 300 s. The electrode dynamics at the electrode surface follow the Butler-Volmer equation. Lithium ion flux follows the Nernst-Planck equation. The concentration diffusion of ions is combined with Fick's law, and mass transfer caused by diffusion and migration is taken into account. The ionic mobility conforms to the Nernst-Einstein equation. The conductivity of the electrode material was set as 1×10^{7} S/m, and the conductivity of the electrolyte was set as 4.5 S/m, respectively. The reactive current density was 10 mA cm^{-2} and the diffusion fact of electrolyte ions was 0.5×10^{-9} m^{2} s^{-1}.

Figures

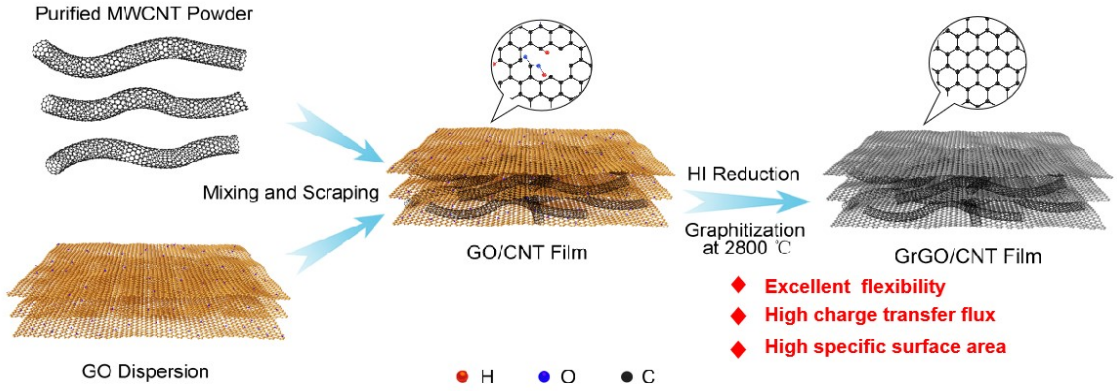

Figure S1 Schematic illustration of preparation of GrGO/CNT film

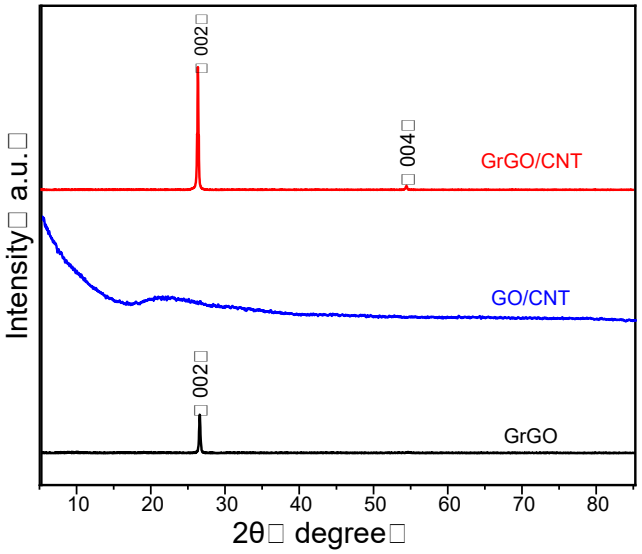

Figure S2 XRD patterns of GrGO, CNT@GO and GrGO/CNT

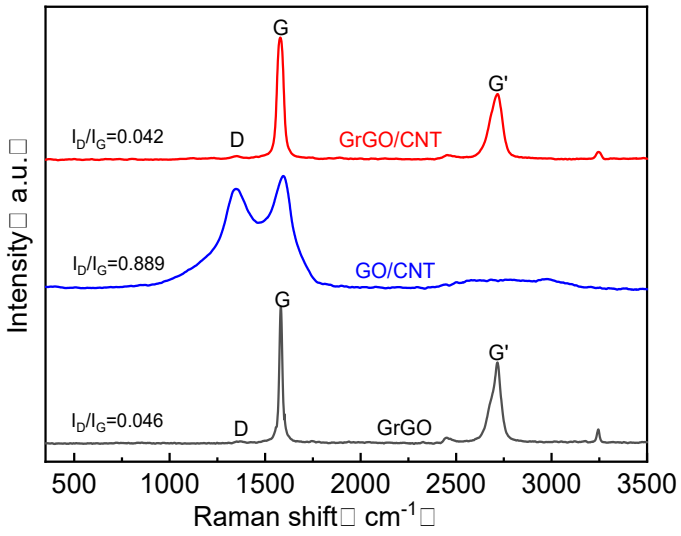

Figure S3 Raman of GrGO, GO/CNT and GrGO/CNT

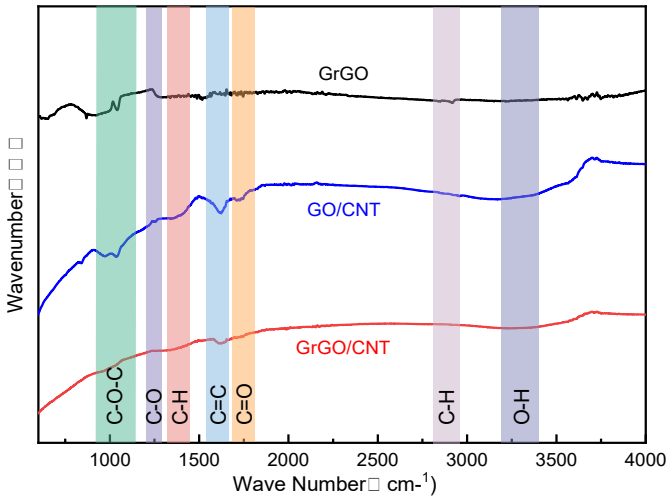

Figure S4 FTIR of GrGO, GO/CNT and GrGO/CNT

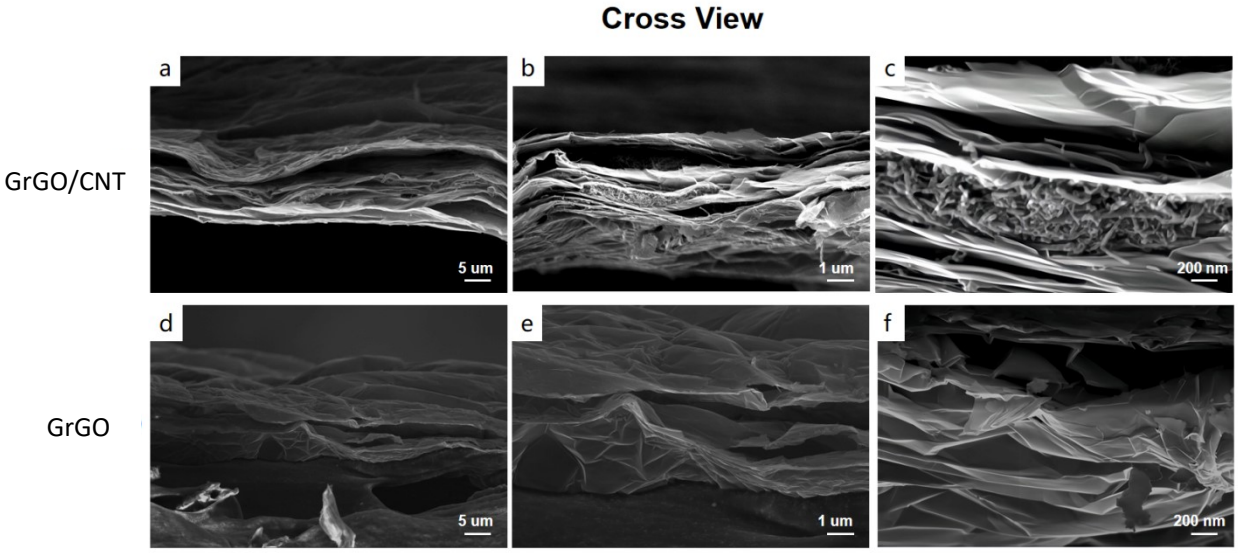

Figure S5 Cross-section images of GrGO and GrGO/CNT film

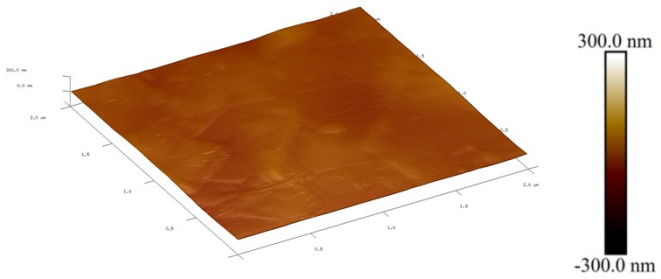

Figure S6 Three-dimensional surface topography map of GrGO/CNT film

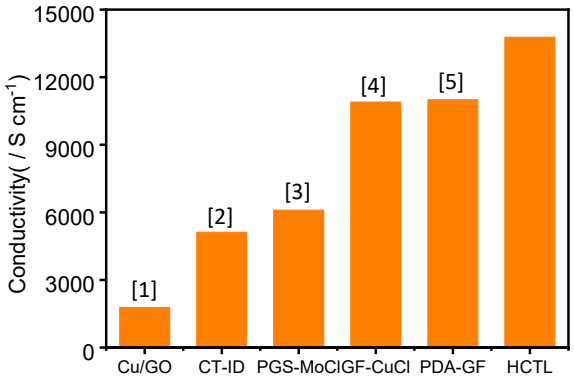

Figure S7 Conductivity comparsion between HCTL film and related carbon materials

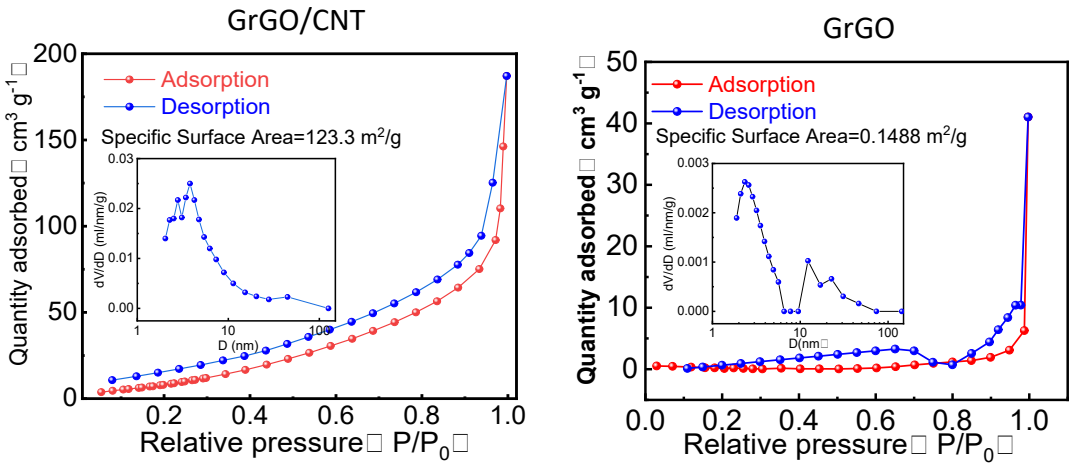

Figure S8 Adsorption/desorption curves and pore size distribution of GrGO and GrGO/CNT film

Table S1 Comparison with recent literature regarding current density, areal capacity, cycling time and voltage hysteresis

Types	Current (mA/cm^2)	Areal capacity (mAh/cm^2)	Time (h)	Voltage (V)
This work	2.5	2.5	2000	0.02
CNTs[6]	1	1	350	0.03
rGO[7]	3	1	140	0.08
Li[8]	1	1	200	0.18
Li/3D-CSC[9]	1	1	2000	0.01
Li@SNC/Li[10]	1	1	1500	0.015
Li@CNFs+CuNPs[11]	1	1	1200	0.01
GN@Cu/Li[12]	0.5	0.5	2100	0.012
VGN/Ni[13]	1	1	2000	0.03
Co-CS/Li[14]	1	1	800	0.05
PP-PTI[15]	1	1	2000	0.05
Li-HrGO-4[16]	1	1	800	0.06
CuFG@Li[17]	1	1	1800	0.03

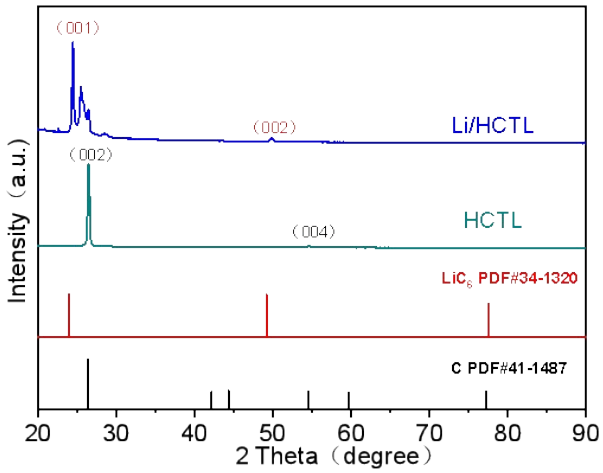

Figure S9 XRD patterns of Li/HCTL

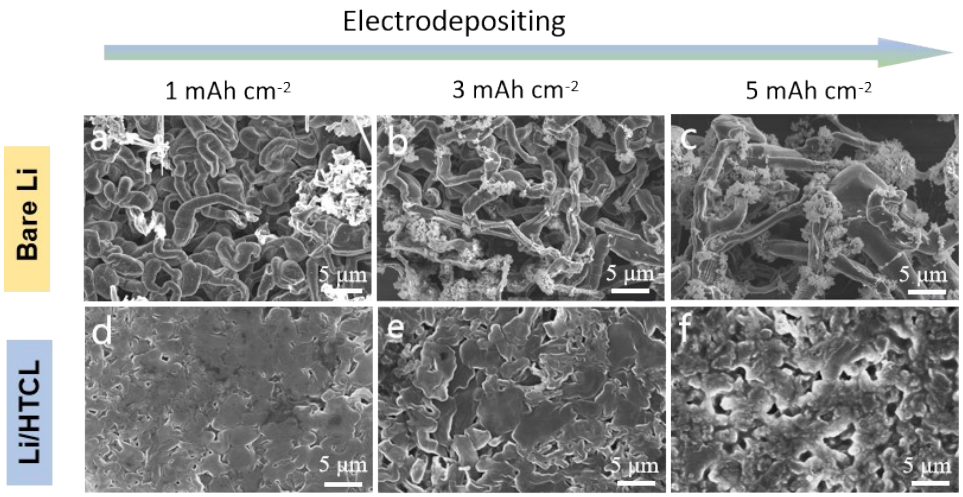

Figure S10 SEM images of bare Li and Li/HCTL depositing with different capabilities of 1, 3 and 5 mAh cm^{-2}

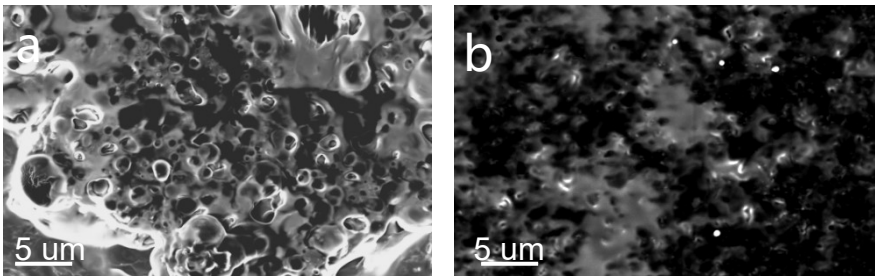

Figure S11 SEM images of (a) bare Li and (b) Li/HCTL electrodes after deposition of 3 mAh cm^{-2} and stripping 1 mAh cm^{-2}

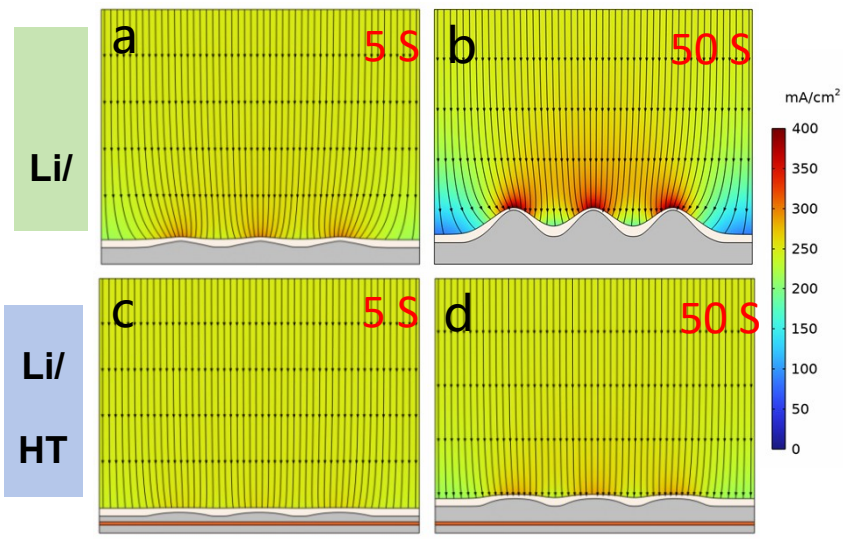

Figure S12 Current disctribution of bare Li and Li/HCTL electrodes deposited with Li simulated by finite element COMSOL method

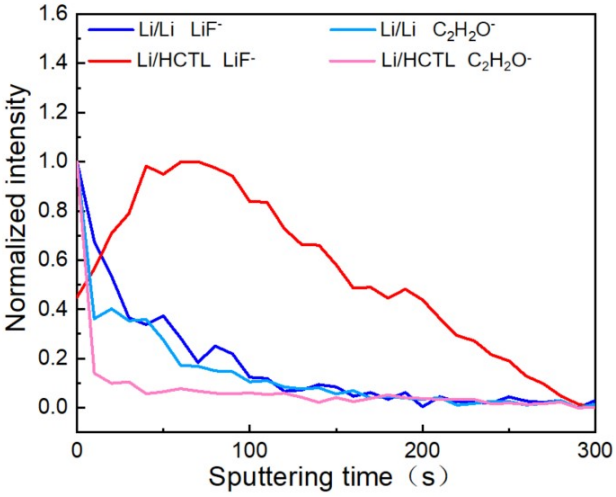

Figure S13 The corresponding TOF-SIMS depth profiles for LiF^- (c) and $C_2H_2O^-$ in the SEI of bare Li and LI/HCTL. Normalized intensity is obtained through log (intensity) conversion.

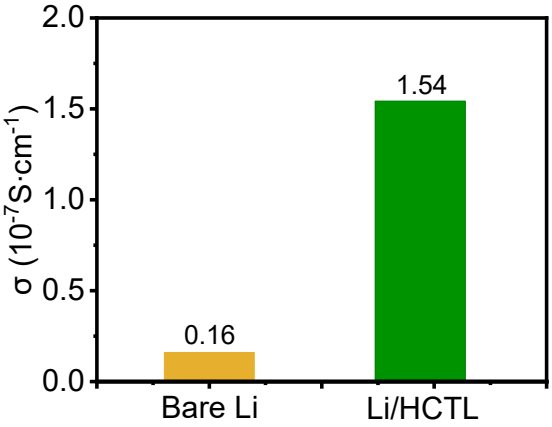

Figure S14 Ion conductivity comparsion of bare Li and Li/HCTL electrodes

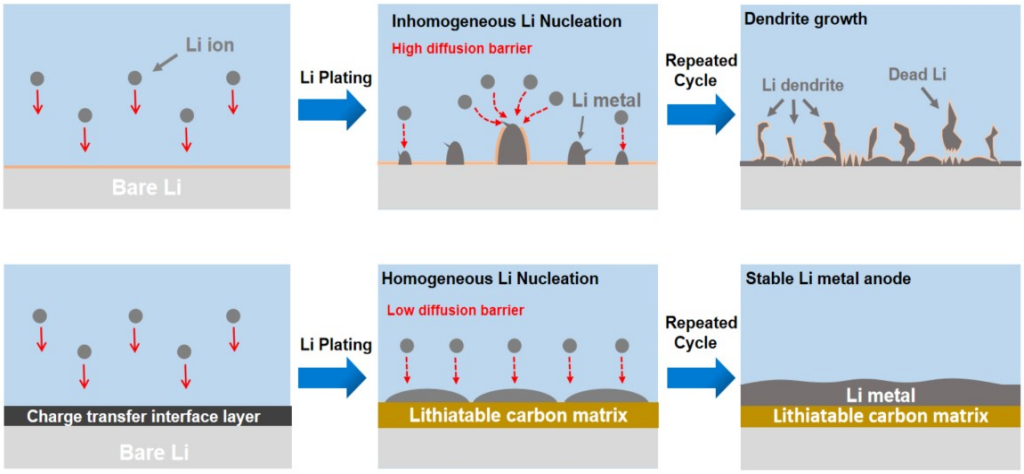

Figure S15 Schematic illustration of depositing mechansim of Li^+ on bare Li and Li/HCTL

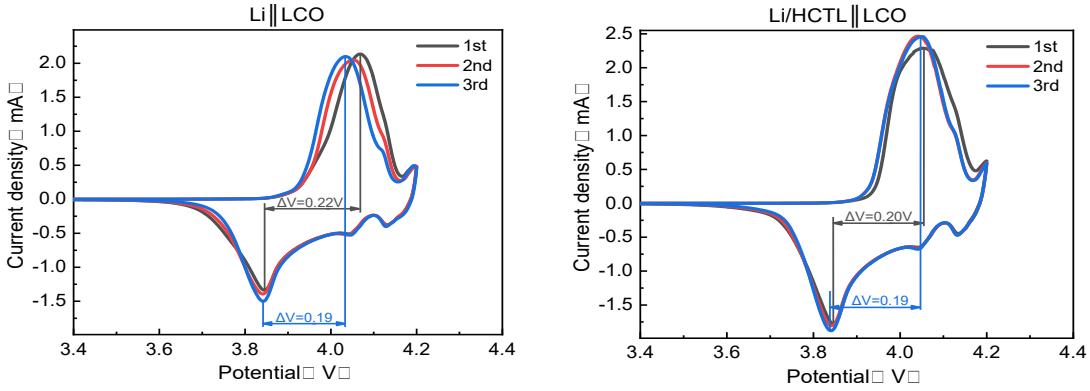

Figure S16 CV curves of Li||LCO and Li/HCTL||LCO at the 1st, 2nd and 3rd cycle

References

[1] P. Shi, T. Li, R. Zhang, X. Shen, X.B. Cheng, R. Xu, J.Q. Huang, X.R. Chen, H. Liu, Q. Zhang. *Adv Mater*. **2019**, 31, 201807131.

[2] M. Mathesh, J. Liu, N.D. Nam, S.K.H. Lam, R. Zheng, C.J. Barrow, W. Yang. *J Mater Chem C*. **2013**, 1, 3084-3090.

[3] I.H. Kim, T. Yun, J.E. Kim, H. Yu, S.P. Sasikala, K.E. Lee, S.H. Koo, H. Hwang, H.J. Jung, J.Y. Park, H.S. Jeong, S.O. Kim. *Adv Mater*. **2018**, 30, 1803267.

[4] K. Pang, X. Liu, Y. Liu, Y. Chen, Z. Xu, Y. Shen, C. Gao. *Carbon*. **2021**, 179, 202-208.

[5] T. Watanabe, A. Itoh, T. Watanabe, T. Kizaki, M. Inaguma, A. Hosoi, H. Kawada. *Carbon*. **2021**, 185, 314-323.

[6] S. Park, H.J. Jin, Y.S. Yun. *Adv Mater*. **2020**, 32, 2002193.

[7] D. Lin, Y. Liu, Z. Liang, H. W. Lee, J. Sun, H. Wang, K. Yan, J. Xie, Y. Cui. *Nat Nanotechnol*. **2016**, 11, 626-632.

[8] K. Liu, Z. Li, W. Xie, J. Li, D. Rao, M. Shao, B. Zhang, M. Wei. *Energy Storage Mater*. **2018**, 15, 308-314.

[9] L. Ye, M. Liao, H. Sun, Y. Yang, C. Tang, Y. Zhao, L. Wang, Y. Xu, L. Zhang, B. Wang, F. Xu, X. Sun, Y. Zhang, H. Dai, P.G. Bruce, H. Peng. *Angew Chem Int Ed*. **2019**, 58, 2437-2442.

[10] M. Chen, J. Zheng, O. Sheng, C. Jin, H. Yuan, T. Liu, Y. Liu, Y. Wang, J. Nai, X. Tao. *J Mater Chem A*. **2019**, 7, 18267-18274.

[11] W. Jia, T. Chen, Y. Wang, S. Qu, Z. Yao, Y. Liu, Y. Yin, W. Zou, F. Zhou, J. Li. *Electrochim Acta*. **2019**, 309, 460-468.

[12] G. Yang, J. Chen, P. Xiao, P.O. Agboola, I. Shakir, Y. Xu. *J Mater Chem A*. **2018**, 6, 9899-9905.

[13] F. Ren, Z. Lu, H. Zhang, L. Huai, X. Chen, S. Wu, Z. Peng, D. Wang, J. Ye. *Adv Funct Mater*. **2018**, 28, 1805638.

[14] S. Li, Q. Liu, J. Zhou, T. Pan, L. Gao, W. Zhang, L. Fan, Y. Lu. *Adv Funct Mater*. **2019**, 29, 1808847.

[15] S. Di, H. Li, B. Zhai, X. Zhi, P. Niu, S. Wang, L. Li. *Proc Natl Acad Sci U S A*. **2023**, 120, e2302375120.

[16] G. Li, X. Shiwei, B. Li, M. Yin, F. Shao, H. Li, T. Xia, Z. Yang, Y. Su, Y. Zhang, J. Ma, J. Yu, N. Hu. *ChemElectroChem*. **2021**, 8, 3273-3281.

[17] W. Zhu, W. Deng, F. Zhao, S. Liang, X. Zhou, Z. Liu. *Energy Storage Mater*. **2019**, 21, 107-114.